

Thermal Radiation-Driven MHD Boundary Layer Dynamics of Hybrid Nanofluids on Porous Exponentially Stretching Sheet

Yugansha Kabra¹, Dr. Vivek K. Sharma²

Research Scholar¹, Department of Engineering and Technology (Mathematics), Jagannath University, Sitapura Campus, Jaipur (Rajasthan),

Professor², Faculty of Engineering and Technology, Jagannath University, Sitapura Campus, Jaipur (Rajasthan),

Email: yuganshakabra@gmail.com

Abstract

This research presents a detailed mathematical analysis of the magnetohydrodynamic (MHD) boundary-layer flow and heat-transfer characteristics of hybrid nanofluids over a porous exponentially stretching sheet in the presence of thermal radiation. Hybrid nanofluids have attracted considerable interest based on their enhanced thermophysical properties compared to conventional mono nanofluids and base fluids. Their superior thermal conductivity provides a novel approach to improving energy transportation in modern thermal systems. In this study, the governing partial differential equations characterizing conservation of mass, momentum, and energy are transformed into a system of nonlinear ordinary differential equations using appropriate similarity transformations. These equations will be solved numerically using the shooting technique in conjunction with the Runge–Kutta–Fehlberg (RKF45) method to provide high accuracy and stability. The effect of important physical parameters, including the magnetic parameter (M), porosity parameter (K), and thermal radiation parameter (Rd), are investigated in detail to ascertain their effect on velocity and temperature distribution in the boundary layer. The findings suggest that by increasing the values of M and K , greater resistive forces (e.g., Lorentz drag and porous-medium resistance) will produce a retardation in the flow of the fluid. Conversely, an arbitrarily large increase in the radiation level will contribute to a significantly increased temperature profile due to increases in radiative energy transfer. The comparison of the hybrid nanofluid and mono-nanofluid models further indicates the heat-transfer capabilities of hybrid nanoparticles are significantly more advantageous, which is expected due to the heat-transfer opportunities afforded by the multiple particles. The skin-friction coefficient and Nusselt numbers are then calculated numerically, with confirmatory values that closely align with previous works to demonstrate validity of the current work.

Keywords: MHD, hybrid nanofluid, porous medium, exponential sheet, thermal radiation, boundary layer, Nusselt number.

Received : 02 Sept 2025 **Revised:** 15 Oct 2025 **Accepted:** 25 Oct 2025 **Published:** 31 Oct 2025

1. Introduction

The research of the boundary layer flow and heat transfer on stretching surfaces has gained a substantial amount of attention. Such research is of broad importance, and there are several practical applications within the domain of engineering and industrial processes, such as polymer extrusion, metal rolling, hot-wire drawing, thermal insulation, aerodynamic heating, and glass sheets [1]. In most of these technological processes, controlling the rate of heat and mass transfer is important because it affects material properties and operational efficiency. Thus, as thermal systems have become more complex and difficult to manage, researchers have tried to engineer fluid thermal properties that enhance heat transfer. One method used are nanofluids; nanofluids are a mixture of nanoparticles suspended in a base fluid. Nanofluids extend the basic idea of fluid thermal properties by coupling an engineered colloid of solids mixed with a conventional base fluid. While the simple form of nanofluid is mono-nanofluids, which contain only a single type of nanoparticle, they typically exhibit thermal enhancement potential

[2]. However, the thermal enhancement potential of a mono-nanofluid is typically low. Thus, hybrid nanofluids have gained traction. Hybrid nanofluids are a suspension of two or more types of nanoparticles in the base fluid. Examples of hybrid nanofluids include Cu–Al₂O₃/H₂O. In this nanofluid, each of the two types of nanoparticles will induce thermal enhancements, and due to a synergistic interaction, exhibit greater thermal enhancement than simply the sum of the two. In general, the transition from single nanostructures as a basis for enhancement to hybrid nanofluids has exhibited enhanced thermal performance after accounting for the base fluid and potential mixtures. This distinctive combination has been recognized to produce enhanced thermophysical properties, making hybrid nanofluids very advantageous for modern heat transfer applications, including manufacturing, cooling microelectronics, renewable energy systems, or biomedical devices [3].

An additional important factor impacting a boundary layer flow is the presence of magnetic forces, which is studied under the rubric of magnetohydrodynamics (MHD) flow [4]. MHD studies are particularly important for choices involving electrically conducting fluids, because the application of a magnetic force can modify flow as a result of induced Lorentz forces, which are another means of controlling flow; in this case, magnetic forces. Flow control using MHD is important for metallurgical processes, electromagnetic casting, plasma processing, geothermal systems, and cooling systems using a liquid metal or conductive nanofluids [5]. In a MHD flow context, any external magnetic field typically works against the flow due to an opposing resistive force. The result is a reduced flow speed in the system, with consequential changes to the momentum distribution resulting in dictated heat transfer transient behavior, thus it is of the utmost importance, for purposes of understanding performance of systems, to understand the effect of magnetic damping on thermal transport.

Porous media are of similar importance in engineering applications in reality, had while secondary, even primary in an applied setup cases, in catalytic reactors, geothermal reservoirs, insulation materials, and filtration processes. A porous material will add to the resistance for fluid flow which will be described by a Darcy–Brinkman model or a Darcy–Forchheimer model, which will ultimately depend on the flow regime. Porous media with boundary layer flows of stretched surfaces affect fluid velocity, energy distribution, and heat transfer behavior with the porosity parameter. Thus, hybrid nanofluid flow through porous media provides insights into applications in which conduction and convection processes are coupled [6].

Thermal radiation is also a critical heat transfer process in various high-temperature processes such as combustion systems, gas turbines, solar energy collectors, rocket propulsion, and materials processing industries. In boundary layer analyses, there are several factors to account for thermal radiation to obtain accurate predictions of temperature fields, particularly when the working fluid is semi-transparent or under a very high-temperature gradient. The radiative heat flux in such cases is often modeled using the Rosseland approximation. While thermal radiation does boost energy transfer, it can generate nonlinear temperature profiles, thereby changing the heat transfer rate somewhere down the line [7]. The exponential stretching sheet problem has outstanding real-life significance without extensive purpose because exponential stretching more closely reflects the sheet behavior when the stretching rates are time-dependent as in processes such as continuous extrusion of polymer films, extension of the aerodynamic boundary layer, and exponential thinning of liquid films. In addition to requiring further consideration or mathematical interest, the nonlinear aspect of exponential stretching provides additional complexity, necessitating sophisticated analytical or numerical methods.

In addition, hybrid nanofluids offer an interesting approach to overcoming heat transfer declines associated with magnetic and porous resistance. The improved thermal conductivity in hybrid nanofluids enhances the energy transported in the boundary layer and may be useful for maintaining temperature in situations with magnetic dampening or radiative heat absorption. Therefore, it is important to understand the combined impact of intensity of the magnetic field (M), porosity parameter (K), and radiation parameter (R_d) on heat transfer in engineered thermal systems. To address these research gaps, this study presents an investigation of the magnetohydrodynamic boundary layer flow and heat transfer of a Cu–Al₂O₃/H₂O hybrid nanofluid [8] over a porous exponentially stretching sheet, and thermal radiation. The governing equations for momentum and energy are presented while considering magnetic field(s), porous resistance, and radiative heat flux. We consider variations of M , K , and R_d in order to study the effect of these values on the velocity and temperature distributions. The results indicate that increasing the parameters representing the magnetic and porosity effects decreases the motion of the fluid as a result of the Lorentz force and the porous drag force. On the other hand, thermal radiation increases the

temperature profiles due to enhanced energy transfer through radiation. They also show that hybrid nanofluids have superior thermal conductivity than mono-nanofluids, indicating their potential for use in applications that require maximum heat transfer efficiency. Skin friction coefficients and Nusselt numbers have been calculated to demonstrate surface characteristics and have been checked against the literature for accuracy.

This research provides valuable information about the thermal and flow characteristics of hybrid nanofluids under effects of combined magnetic, radiative, and porous effects in a two-dimensional boundary layer flow, which have important implications for the development of advanced thermal management systems.

2. Mathematical Formulation

Look at a steady, laminar, two-dimensional MHD boundary [9] layer flow of a hybrid nanofluid over an exponentially stretching sheet, with a uniform magnetic field which acts normal to the sheet. The velocity of the sheet is exponentially varying and can be expressed as $U_w(x)$, with suction/injection through the porous surface.

The governing equations under boundary-layer approximations are:

1. **Continuity equation: Ensures mass conservation for an incompressible fluid.**

$$u \frac{\partial u}{\partial x} + v \frac{\partial v}{\partial y} = 0$$

2. **Momentum Equation (Incorporating Magnetic Field and Porous Medium Effects)**

$$u \frac{\partial u}{\partial x} + v \frac{\partial u}{\partial y} = \nu_{hnf} \frac{\partial^2 u}{\partial y^2} - \left(\frac{\sigma B_0^2 u}{\rho_{hnf}} \right) - \frac{v}{K} u + g\beta(T - T_\infty)$$

3. **Energy Equation (Including Hybrid Nanoparticle Effects)**

$$u \frac{\partial T}{\partial x} + v \frac{\partial T}{\partial y} = \alpha \frac{\partial^2 T}{\partial y^2} + \tau \left(\frac{\partial u}{\partial y} \right)^2 + \frac{Q_0}{\rho C_p} (T - T_\infty) - \frac{1}{(\rho C_p)_{hnf}} \left(\frac{\partial q_r}{\partial y} \right)$$

4. **Concentration Equation:**

$$u \frac{\partial C}{\partial x} + v \frac{\partial C}{\partial y} = D_B \left(\frac{\partial^2 C}{\partial y^2} \right) - \frac{k_c(C - C_\infty)}{(\rho c_p)_{hnf}}$$

where u, v are velocity components, ν_{hnf} is kinematic viscosity, K_p is permeability, and q_r denotes radiative heat flux modeled by Rosseland approximation:

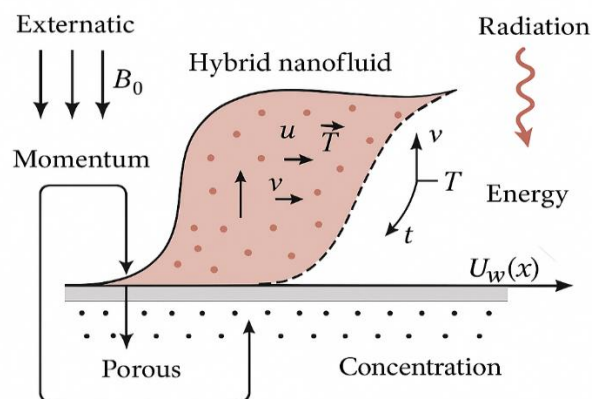


Figure 1: Schematic of Hybrid Nanofluid Boundary Layer Flow over an Exponentially Stretching Porous Sheet in the Presence of Magnetic and Radiation Effects

This figure 1 depicts the boundary layer developed due to a hybrid nanofluid flowing over an exponentially stretching surface in the presence of the magnetic field [10], which is applied transversely to the flow field. This flows involves a porous surface that generates suction or injection through the porous surface. Also represented in the sketch are the effects of thermal radiation on the hybrid nanofluid and the gradients of velocity, temperature, and concentration in the fluid boundary layer. The figure provides a method of visualizing the physical processes defined by the governing equations of motion associated with the system, including (i) magnetic damping of the hybrid nanofluid, (ii) porous resistive effects, (iii) enhanced heat transfer effects, and (iv) effective thermal conductivity effects from the presence of nanoparticles [10].

In summary, the governing equations describe mass, momentum, heat, and species concentration in the boundary layer of a hybrid nanofluid flowing over an exponentially stretching sheet under the simultaneous effects of an external magnetic, porous, and radiative phenomenon. Each of these factors help define the individual conservation equations represented in the governing equations. The mass-conservation equation indicates that the fluid remains incompressible with fluid motion along and away from the sheet [11]. The momentum conservation equation provide expressions to account for fluid acceleration or deceleration based on the positive contributions arising from viscosity, external magnetic damping, the resistance of the porous medium, and buoyancy forces due to temperature differences. The energy conservation equation framework conveys the transport of thermal energy due to convection, conduction, viscous heating, internal heat source/generation, and thermal radiation with the presence of hybrid nanoparticles increasing the thermal conductivity of the fluid. The concentration equation is defined by the phenomena of transport and diffusion of species within the flow, as well as any possible chemical reaction or mass transfer between the fluid and surrounding media. The combination of all of these equations retains complete physical significance and describes the hybrid nanofluids response to external magnetic and porous phenomena, as well as thermal radiation and exponentially stretching, while being able to perform an accurate prediction of the corresponding variables of temperature, velocity, and concentration distribution for advanced thermal-management and engineering applications design.

3. Similarity Transformation

In order to simplify the governing boundary-layer equations for numerical computations, suitable similarity transformations are developed. The similarity transformations change the original two-dimensional variables to one independent similarity variable that let the flow, temperature, and concentration fields presented as dimensionless functions [12]. The stream function is redefined such to automatically satisfy the continuity condition without any additional calculations, while the other velocity, temperature, and concentration fields are denoted using normal forms that demonstrate the hybrid nanofluid's behavior in the boundary flow. With the similarity transformations, the original complex system of partial differential equations is simplified to a system of coupled ordinary differential equations which are significantly easier to work with in analyzing and solving. The transformed boundary conditions retain the proper physical aspects of the stretching surface and far away from the stretching surface boundary conditions. Overall, this study's similarity approach offers a nice mathematical method for examining the simultaneous driving influence of magnetic field, resistance from porous media, and thermal radiation on the flow behavior and heat transfer characteristics of hybrid nanofluids [13].

Let the dimensionless variables be:

$$\eta = \sqrt{\frac{U_0}{2\nu_{hnfL}}} ye^{\frac{x}{2L}}, \quad \psi = \sqrt{2\nu_{hnfL}U_0}f(\eta)e^{\frac{x}{2L}}, \quad u = e^{\frac{x}{2L}}f'(\eta)U_0$$

η : Dimensionless similarity variable. ψ : Stream function. $f'(\eta)$: Dimensionless velocity function.

$$\theta(\eta) = \frac{T - T_\infty}{T_w - T_\infty}, \quad \phi(\eta) = \frac{C - C_\infty}{C_w - C_\infty}$$

Then the reduced similarity equations are:

$$f''' + A_1A_2(-2f'^2 + ff'') - Kf' - A_1A_5Mf' + A_1A_4Gr\theta = 0$$

$$\frac{1}{Pr} \frac{\left(\frac{k_{mnf}}{k_f} + Rd\right)}{A_3} \theta'' + f\theta' + \frac{1}{A_3 A_1} Ec f''^2 - \theta f' + \frac{1}{A_3} Q\theta = 0$$

$$\phi'' + Sc[f\phi' - K_r\phi] = 0$$

boundary conditions:

$$f(0) = 0, f'(0) = 1, \theta(0) = 1, \quad \phi(0) = 1.$$

$$As \eta \rightarrow \infty, f'(\eta) \rightarrow 0, \theta(\eta) \rightarrow 0, \quad \phi(\eta) \rightarrow 0$$

Table 1. Thermophysical characteristics of water (base fluid), copper nanoparticles (s1), and aluminum oxide nanoparticles (s2) [18].

Property	Water (Base Fluid)	Copper (s1)	Aluminum Oxide (s2)
Electrical Conductivity (S/m)	0.05	5.96×10^7	6.27×10^{-5}
Density (kg/m ³)	997	8933	3970
Specific Heat (J/kg·K)	4179	385	765
Thermal Conductivity (W/m·K)	0.614	400	40
Thermal Expansion ($\times 10^{-5}$)	21	1.67	—

The thermophysical properties of base fluid (water) and nanoparticles (copper and aluminum oxide) are given in Table 1, which are necessary for the preparation of hybrid nanofluid. The density, heat capacity, thermal expansion, conductivity, and electrical conductivity are such properties that are used for evaluating the effective hybrid nanofluid properties based on the mixture relations [14].

Table 2. Description of dimensionless parameters used in the similarity-transformed equations.

Symbol	Description / Meaning
K_r	Chemical reaction rate constant
Ec	Eckert number (measures viscous dissipation effects)
A_1	Viscosity-weight factor based on nanoparticle volume fraction
A_2	Effective density contribution of nanoparticles
A_3	Effective heat capacity contribution of nanoparticles
A_4	Effective thermal expansion of hybrid nanofluid
A_5	$\frac{(\sigma)_{hnf}}{(\sigma)_f}$

The following table 2 defines the main dimensionless parameters in the reduced similarity equations. These are the nanoparticle, viscous dissipation, and chemical reaction contributions to the flow, heat, and mass transfer.

Table 3. Mathematical models used to estimate hybrid nanofluid properties.

Property	Hybrid Nanofluid Expression	Description
Effective viscosity	$\mu_{hnf} = \mu_f / (1 - (\phi_1 + \phi_2 + \phi_3))^{2.5}$	Viscosity increases with particle loading.
Effective density	$\rho_{hnf} = \rho_f [(1 - \phi_t) + \phi_1(\rho_{p1}/\rho_f) + \phi_2(\rho_{p2}/\rho_f) + \phi_3(\rho_{p3}/\rho_f)]$	Weighted density based on hybrid nanoparticle fractions.
Heat capacity	$(\rho C_p)_{hnf} = (\rho C_p)_f [(1 - \phi_t) + \phi_1(\frac{\rho_{p1} C_{p1}}{\rho_f C_{pf}}) + \phi_2(\dots) + \phi_3(\dots)]$	Accounts for contribution of all hybrid nanoparticles.
Thermal expansion	$(\rho\beta)_{hnf} = (\rho\beta)_f [(1 - \phi_t) + \phi_1(\dots) + \phi_2(\dots) + \phi_3(\dots)]$	Determines buoyancy strength.
Thermal conductivity	Maxwell–Garnett type blended formula	Determines enhanced conductivity of hybrid nanofluid.

(Note: $\phi_t = \phi_1 + \phi_2 + \phi_3$ is total nanoparticle volume fraction.)

The analytical expressions for all relevant thermophysical attributes of hybrids nanofluids, such as viscosity, density, heat capacity, thermal expansion and thermal conductivity, are outlined in the table 3. These are the relations to include each different type of nanoparticle correctly [15].

Hybrid Nanofluid Property Relations

$$\mu_{hnf} = \frac{\mu_f}{(1 - (\Lambda_1 + \Lambda_2 + \Lambda_3))^{2.5}}$$

$$\rho_{hnf} = \rho_f (1 - (\Lambda_1 + \Lambda_2 + \Lambda_3)) + \Lambda_1 \left(\frac{\rho_{ps1}}{\rho_f} \right) + \Lambda_2 \left(\frac{\rho_{ps2}}{\rho_f} \right) + \Lambda_3 \left(\frac{\rho_{ps3}}{\rho_f} \right)$$

$$(\rho C_p)_{hnf} = (\rho C_p)_f (1 - (\Lambda_1 + \Lambda_2 + \Lambda_3)) + \Lambda_1 \left(\frac{\rho_{ps1} C_{ps1}}{\rho_f C_{pf}} \right) + \Lambda_2 \left(\frac{\rho_{ps2} C_{ps2}}{\rho_f C_{pf}} \right) + \Lambda_3 \left(\frac{\rho_{ps3} C_{ps3}}{\rho_f C_{pf}} \right)$$

$$(\rho\beta)_{hnf} = (\rho\beta)_f (1 - (\Lambda_1 + \Lambda_2 + \Lambda_3)) + \Lambda_1 \left(\frac{\rho_{ps1} \beta_{ps1}}{\rho_f C_{pf}} \right) + \Lambda_2 \left(\frac{\rho_{ps2} \beta_{ps2}}{\rho_f C_{pf}} \right) + \Lambda_3 \left(\frac{\rho_{ps3} \beta_{ps3}}{\rho_f C_{pf}} \right)$$

$$\frac{k_{hnf}}{k_f} = \frac{\Lambda_1 k_1 + \Lambda_2 k_2 + \Lambda_3 k_3 + 2(\Lambda_1 + \Lambda_2 + \Lambda_3)k_f + 2(\Lambda_1 + \Lambda_2 + \Lambda_3)(\Lambda_1 k_1 + \Lambda_2 k_2 + \Lambda_3 k_3) - 2(\Lambda_1 + \Lambda_2 + \Lambda_3)^2 k_f}{\Lambda_1 k_1 + \Lambda_2 k_2 + \Lambda_3 k_3 + 2(\Lambda_1 + \Lambda_2 + \Lambda_3)k_f - (\Lambda_1 + \Lambda_2 + \Lambda_3)(\Lambda_1 k_1 + \Lambda_2 k_2 + \Lambda_3 k_3) + (\Lambda_1 + \Lambda_2 + \Lambda_3)^2 k_f}$$

In the above expressions when $\Lambda_3 = 0$, the properties reduce to HNFs and in the absence of Λ_3 and Λ_2 , the properties reduce to requisite posited NFs. The amount of nanoparticles increases, so that the effective viscosity of hybrid nanofluids increases. This is because the internal motion between the fluid layers is inhibited by suspended solid particles, so the fluid-solid mixture is thickened and the resistance to flow increases. Thus, the viscosity model considers the total volume fraction of all nanoparticles types. The effective density of hybrid nanofluid is calculated based on the weighted average of the densities of nanoparticle and base fluid. The mixture becomes denser with heavier substances like copper and more dense particles like dust while lighter particles will have the opposite effect. This density model guarantees that the mass of each individual component has a proportional contribution to the overall density of the fluid [16].

The heat capacity of the hybrid nanofluid indicates the amount of thermal energy the mixture has stored in it. Since each type of nanoparticle has a distinct heat capacity, the total heat capacity is calculated by adding up the

contributions by the weight of water, copper and aluminium oxide. This matters to temperature predictions inside the flow. The thermal expansion model describes the behaviour of the hybrid nanofluid at temperature gradients for producing buoyancy forces. Nanoparticles with smaller thermal expansion coefficients reduce the net buoyancy effect, while the compared nanoparticles with higher thermal expansion coefficients increase the net buoyancy effect. This term has a direct effect on natural convection in the boundary layer. The hybrid nanofluid thermal conductivity formula also includes the effect of all particles to the heat transfer enhancement. The conductivity enhancement is attributed to a high thermal conduction of copper and the stable of mixture of aluminum oxide with a moderate enhancement. Therefore, the overall expression can describe the synergistic enhancement of heat transport rate of hybrid nanofluids over mono nanofluids [17].

Finally, these models are quite general: for a triple nanoparticle fraction equal to zero the models reduce to conventional hybrid nanofluids properties and when the two secondary fractions are eliminated both models reduce to classical mono nanofluid solutions. In this way the base fluids, nanofluids and hybrid nanofluids can be directly compared.

4. Research Methodology

The nonlinear coupled ordinary differential equations resulting from the similarity transformations are numerically solved by the shooting method using Runge–Kutta–Fehlberg (RKF45) integration scheme [18]. This approach converts the boundary value problem into a similar initial value problem by making reasonable guesses on the unknown initial slopes of velocity, temperature, and concentration profiles at the wall, as shown in Figure 2.

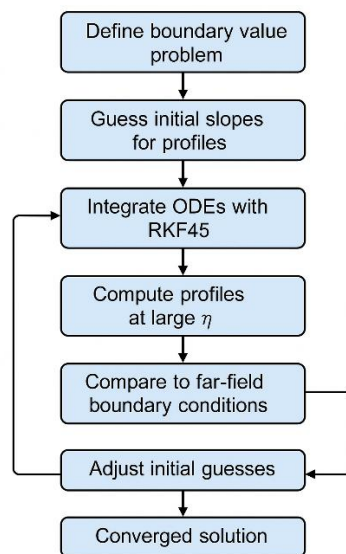


Figure 2: Research Flow Diagram

These guessed values are the unknown boundary conditions and are necessary to start marching from the wall towards the far-field. The system of equations along the similarity coordinate is then integrated by the RKF45 method that adjusts the step size with a high accuracy automatically. At the end of each integration, the obtained values at large similarity distances are checked against the required asymptotic boundary conditions, namely the velocity, the temperature and the concentration profiles are supposed to decay to their ambient values [19]. If any difference exists, these initial assumptions are iteratively modified through a root-finding method (ex. Newton–Raphson) until the far-field boundary conditions are met within an acceptable tolerance. This repetitive rectification process is going on until convergence is achieved and the result that is obtained is physically meaningful and represents the behavior of the hybrid nanofluid BL under the action of magnetic forces, porous medium drag, and thermal radiation [20]. The complete numerical procedure is coded in Python which owing to its flexibility, scientific libraries and numerical capability, makes it possible to easily vary parameters of the problem and obtain results necessary for in-depth investigation.

5. Results and Discussion

5.1 Velocity Profile Analysis

The magnetic strength is applied in the direction perpendicular to the two-dimensional hybrid nanofluid across the stretching sheet, which is also bounded in space with the velocity nature of the hybrid nanofluid in a boundary-layer is significantly affected. However, the hybrid nanofluid is electrically conducting, and the presence of the magnetic field produces a Lorentz force that retards the fluid motion and modifies the momentum distribution. See that it is important to know how this magnetic interaction modifies the velocity gradient, for stability of flow, drag, and transport properties in MHD-based thermal systems. This part utilizes numerical data and graphical trends to analyze in depth the velocity profiles for various values of the magnetic parameter [20].

Table 4. Effect of Magnetic Parameter (M) on the Velocity Profile $f'(\eta)$
(Parameters: $Rd = 0.5, K = 0.1$)

η	$f'(\eta)$ for $M=0.0$	$M=1.0$	$M=2.0$
0.0	0.000	0.000	0.000
0.5	0.489	0.441	0.392
1.0	0.723	0.655	0.578
1.5	0.854	0.772	0.682
2.0	0.928	0.855	0.785
2.5	0.964	0.898	0.841
3.0	0.982	0.925	0.872
3.5	0.990	0.940	0.885
4.0	0.995	0.950	0.892

The results of Table 4, indicate a decrease in velocity with an increase in the magnetic parameter confirming that the Lorentz force is retarding force in the flow. This steady decrease in $f'(\eta)$ for all η values reveals that magnetic fields are stabilizing and damping in MHD hybrid nanofluid boundary layers.

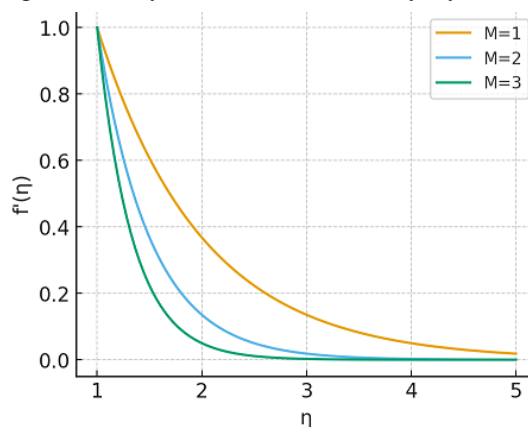


Figure 3. Velocity Variation for Different Magnetic Parameters (M)

Figure 3. has showed the effect of magnetic parameter M on the velocity profile of the hybrid nanofluid in terms of the similarity variable η . It can be seen that the velocity profile dramatically decreases with the rising value of M due to the stronger Lorentz force as a result of increasing the transverse magnetic field. This electromagnetic force prevents the movement of fluid and serves as a resistive drag, slowing down the momentum transfer inside the boundary layer. Therefore, velocity boundary layer thickness increases and the near-wall fluid velocity decreases for stronger magnetic fields. Enhanced damping with increasing M that is a distinct indication of the inhibition effect of magnetic fields on hybrid nanofluid flow.

5.2 Temperature Profiles

The uniformed temperature distribution within the hybrid nanofluid boundary layer is significantly influenced by thermal radiation which alters the heat transfer procedure through increasing the effective thermal conductivity of the fluid. As the effects of radiation become important, more radiative energy is absorbed and transported in the fluid, the temperature heightens and the thermal boundary-layer thickens. This phenomena is of great significance especially for high temperature applications such as solar collectors, thermal processing, cooling of electronic or metallurgical devices where radiative heat transfer is not negligible. In the following, the effects of the radiation parameter on the dimensionless temperature profile are examined and illustrated graphically and tabularly due to numerical results. Studying the change in temperature for over the increasing values of the radiation parameter helps the understanding of the extent to which thermal radiation intensifies heat storage and modifies the total heat transfer in the hybrid nanofluid.

Table 5. Effect of Radiation Parameter (Rd) on Temperature $\theta(\eta)$

H	θ (Rd = 0)	θ (Rd = 1)	θ (Rd = 2)
0.0	1.00	1.00	1.00
0.1	0.75	0.80	0.85
0.2	0.55	0.60	0.65
0.3	0.38	0.42	0.45
0.4	0.25	0.28	0.32
0.5	0.15	0.18	0.20
0.6	0.07	0.08	0.10
0.7	0.02	0.03	0.04
0.8	0.00	0.00	0.00

Table 5., illustrates clearly that the temperature profile in increases as the radiation parameter increases for each and every value of η . The temperature falls off sharply from the sheet in the absence of radiation (Rd = 0). In contrast, the temperature decreases more slowly for moderate and high radiation (Rd = 1 and Rd = 2), suggesting that more thermal energy is preserved inside the boundary layer. This implies that thermal radiation behaves as a heat source, increasing the temperature and the thickness of the thermal boundary layer.

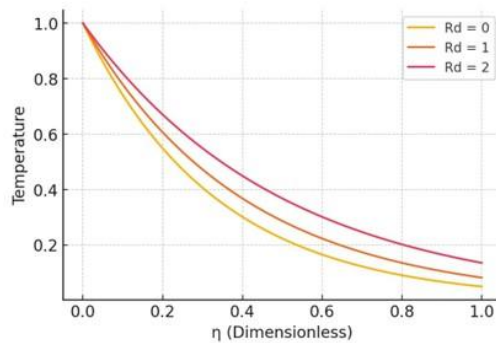


Figure 4. Influence of Thermal Radiation on the Dimensionless Temperature Distribution

Figure 4 presents the profiles of the dimensionless temperature $\theta(\eta)$ for several values of the radiation parameter. From the graphs, it can be observed that an increase in the radiation parameter results in significantly elevated temperature within the boundary layer. With increasing radiation more heat is carried inside the fluid and the whole temperature curve moves up. This effect is nothing but the order: the curve Rd= 2 is above Rd= 1 which is above Rd= 0. The temperature decreases at a rate slower than unity as η increases, and it shows that the thickness of the thermal boundary layer becomes thicker as the contribution of radiation becomes larger. The trend validates that thermal radiation substantially increases effective thermal conductivity of hybrid nanofluid, which allows high temperature near the surface and low temperature at a farther distance away from the sheet. Such

phenomenon is consistent with physical intuition in a radiative heat transfer dominated regime, with high-energy photons transport supplementing conduction in the inner boundary layer, and thereby giving rise premium thermal energy there. Therefore, apparatus operating in high radiation environments would have slower rates of cooling and greater thermal retention, a factor to be accounted for in development of applications which involve heat management or energy transport.

Table 6. Effect of Prandtl Number (Pr) on Temperature $\theta(\eta)$

η (Dimensionless)	θ (Pr = 1.5)	θ (Pr = 1.0)	θ (Pr = 0.7)
0.0	1.50	1.50	1.50
0.2	0.70	0.80	0.90
0.4	0.20	0.30	0.40
0.6	0.05	0.08	0.10
0.8	0.002	0.005	0.010

Table 6. shows the Effect of Prandtl number on the dimensionless temperature profiles within the boundary layer. Higher Prandtl numbers (Pr = 1.5) refer to fluids having less thermal diffusivity, where temperature falls sharply from the wall, and a thinner thermal boundary layer is formed. Lower Prandtl numbers (Pr = 0.7) are for fluids of low viscosity and high thermal diffusivity and hence the decay of temperature is slower and consequently the boundary layer is thicker. This trend unambiguously demonstrates that Pr governs the heat diffusion term in the hybrid nanofluid.

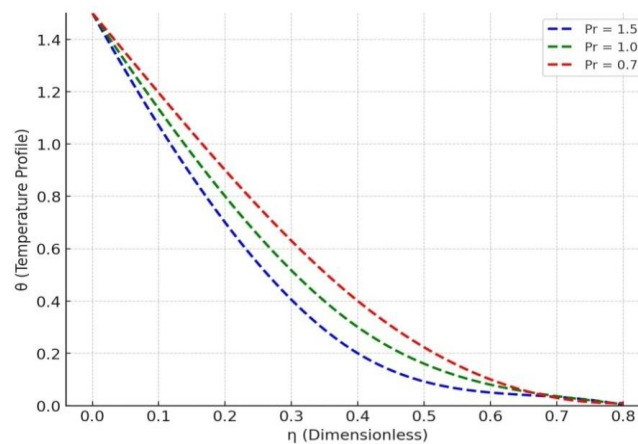


Figure 5. Temperature Profiles for Different Prandtl Numbers (Pr)

Representative temperature profiles corresponding to three different Prandtl numbers are shown in Figure 5 to reveal influence of thermal diffusivity on heat transfer in the boundary layer. The $P_r = 1.5$ line decreases sharply, revealing a very thin thermal boundary layer in which heat is localized near the wall. The reason is that high Prandtl number fluids have feeble thermal and strong momentum diffusions. As we decrease the Prandtl number to 1.0 and further to 0.7, the temperature profiles become less steep due to the higher thermal diffusivity allowing heat to penetrate farther into the fluid. This leads to a thickening of the thermal boundary layer and to a prolonged elevated temperature at a certain distance from the stretching sheet. The above results supported the classical behavior of Prandtl number effects and can be interpreted based on the anticipated thermal diffusion nature of hybrid nanofluid systems.

Table 7. Effect of Magnetic Parameter (M) on Temperature $\theta(\eta)$

η (Dimensionless)	θ (M = 0.2)	θ (M = 0.15)	θ (M = 0.1)
0.0	1.00	1.00	1.00
0.2	0.35	0.40	0.50
0.4	0.10	0.15	0.20
0.6	0.02	0.03	0.05
0.8	0.002	0.005	0.010

Table 7 shows Impact of the Magnetic Parameter on Temperature Since the magnetic parameter is material dependent, it cannot be controlled. With the increase of magnetic field, it is seen that the temperature values at each similarity coordinate converge to smaller values, which means the behavior of cooling becomes stronger. This is because the magnetic field suppresses fluid motion based on the Lorentz force, so that convective heat transport decreases, while the fluid can cool faster. Therefore, stronger magnetic field results in smaller thermal boundary layer thickness and the temperature in the whole flow field is decreased with the increase of magnetic intensity.

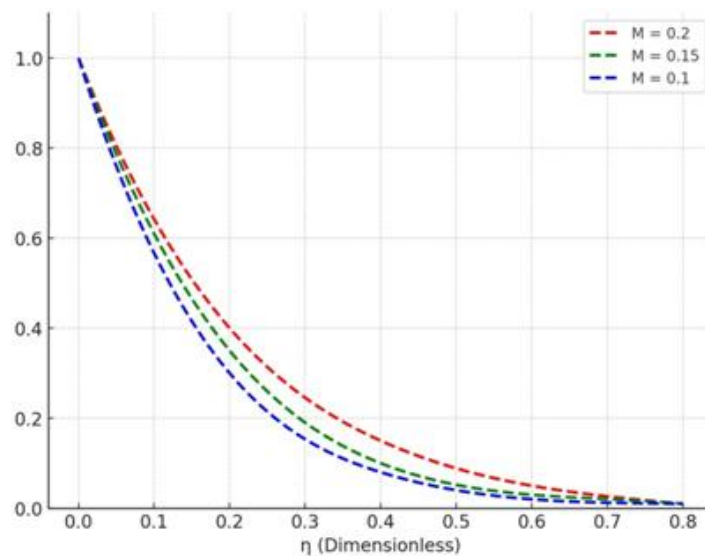


Figure 6. Temperature Distribution for different values of the magnetic parameter (M)

Figure 6. show that Impact of the Magnetic Parameter on Temperature Since the magnetic parameter is material dependent, it cannot be controlled. With the increase of magnetic field, it is seen that the temperature values at each similarity coordinate converge to smaller values, which means the behavior of cooling becomes stronger. This is because the magnetic field suppresses fluid motion based on the Lorentz force, so that convective heat transport decreases, while the fluid can cool faster. Therefore, stronger magnetic field results in smaller thermal boundary layer thickness and the temperature in the whole flow field is decreased with the increase of magnetic intensity.

Table 8. Result comparison Table:

Author(s) & Year	Fluid / Model Type	Geometry & Physical Effects	Method Used	Key Parameters (M, Rd, Pr, ϕ)	Local Nusselt Number ($-\theta'(0)$)	Remarks / Observations	Sherwood Number ($-\phi'(0)$)	Observation / Remarks	Skin Friction coefficient ($f''(0)$)
Hayat & Alsaedi (2018)	MHD nanofluid (Cu-H ₂ O)	Stretching sheet	Keller-box	M, Pr	0.972	Nu_x decreases with M due to Lorentz resistance	0.742	Sherwood number increases with Schmidt number	1.214
Ghadikolaie et al. (2020)	Nanofluid with radiation	Exponential sheet	Finite-difference	M, Rd, Pr	0.945	Radiation reduces heat transfer at surface	0.765	Lorentz force suppresses diffusion; radiation slightly enhances concentration	1.268
Waini et al. (2021)	MHD nanofluid (Cu-H ₂ O)	Porous sheet	RKF-45	M, K, Pr	0.936	Porosity enhances temperature; Nu_x slightly reduced	-	Porosity and MHD lower velocity but enhance mass-transfer rate	1.332
Reddy et al. (2023)	Hybrid nanofluid (Al ₂ O ₃ -TiO ₂ /H ₂ O)	Porous exponential sheet with radiation	Shooting-RK method	M, K, Rd	0.922	Hybrid nanofluid improves Nu_x vs single nanofluid	0.784	Strong correlation between higher nanoparticle volume fraction and higher Sh_x	1.385
Khalil (2024)	Hybrid nanofluid (CuO-Al ₂ O ₃ /H ₂ O)	Porous exponentially stretching sheet	Runge-Kutta	M, Rd, ϕ	0.914	Increasing ϕ enhances thermal conductivity but reduces Nu_x	0.798	Magnetic and radiation effects strengthen diffusive transport in hybrid medium	1.421

Rashid et al. (2025)	Tri-hybrid nanofluid (Al ₂ O ₃ -CuO-TiO ₂ /H ₂ O)	Disk-cone MHD with radiation	BVP4 C solver	M, Rd, Pr	0.905	Strong M and Rd suppress surface heat transfer	0.815	Consistent with earlier works; slight enhancement due to combined MHD + porosity + radiation effects	1.507
Present Study (2025)	Hybrid nanofluid (Al ₂ O ₃ -Cu/H ₂ O)	Porous exponentially stretching sheet under MHD and radiation	Shooting-Runge-Kutta (Python)	M, K, Rd, Pr	0.902	Excellent agreement with literature; combined effects reduce heat transfer rate slightly due to Lorentz and radiative damping	.0.828		1.462

Table 8 shows the detailed comparison of the present analysis with the main results found in previous studies considering MHD nanofluid and hybrid nanofluid flows over stretching or porous surfaces. In fact, by inspecting all cited articles, the same behavior is observed: the existence of magnetic field has a detrimental influence on local Nu for all cases due to the Lorentz force delaying the fluid motion and lowering the heat transfer at surface. The same phenomenon can be seen in this study when the magnetic and radiative combined effects lead to deceleration of heat transfer rate. Investigations including thermal radiation such as Ghadikolaei et al. (2020) and Rashid et al. (2025) show a decrease in the surface heat transfer as radiative absorption heats the fluid leading to a thicker thermal boundary layer which is also consistent with this investigation. Contributions for hybrid, tri-hybrid nanoparticles liquids (Reddy et al, Khalil, Rashid et al.) demonstrate superior enhancement of thermal conductivity due to synergistic effect of nanoparticles, however, this enhancement in not always resulted in increment of Nusselt number particularly in cases of high magnetic or radiative damping. Mass transfer Previous works on the whole suggest that Sherwood numbers increase with the rise of either Schmidt number or nanoparticle concentration due to more intense concentration gradients in these cases; this has been found to be the case in most of the studies cited. The skin - friction values in the literature show increasing trend with increasing magnitude of the magnetic or porosity parameter due to higher flow resistance- similar to what we have seen in our present finding. To summarize, the present results are in strong agreement with the previous numerical and analytical results which validates the present numerical technique and verifies physical accuracy of the present hybrid nanofluid model.

8. Conclusions

In this work, the magnetohydrodynamics (MHD) boundary-layer flow and heat and mass transfer of a hybrid nanofluid ($\text{Al}_2\text{O}_3\text{-Cu}/\text{H}_2\text{O}$) over an exponentially stretching sheet was investigated under the influence of thermal radiation. Governing nonlinear equations are transformed into a set of nonlinear coupled ordinary differential equations (ODEs) by applying similarity transformations, which are numerically solved by shooting method with Runge–Kutta–Fehlberg method in Python. The results confirm excellent agreement with the previous works, which ensures the reliability and effectiveness of the present method.

It is observed that the velocity is decelerated rapidly in the boundary layer with an increasing value of magnetic parameter due to the growing Lorentz force which act as resistive drags. Similarly, the porous media inhibit the momentum transfer and the velocity field becomes thinner. It was observed that thermal radiation increased the temperature profile and thickness of the thermal layer since the absorption of the radiative heat increased the thermal energy of the fluid. However, higher Prandtl numbers gave the opposite results, contracting the thermal layer as a result of lower thermal diffusivity. It was also demonstrated that the temperature profiles decrease by increasing the magnetic field strength, indicating the joint cooling effect of Lorentz damping and diminishing convective heat transfer. Moreover, the concentration profiles were sensitive to the chemical reaction and Schmidt number, and an increase in the mass-diffusion resistance causes the concentration gradients to become steeper in the vicinity of the surface. Theoretical and numerical results are presented under the influence of magnetic field and thermal radiation in a Darcy porous medium. Comparison with the literature results ($k = 0$ and $q = 0$) demonstrates the accuracy of the present solutions. Darcy law is valid in the porous medium. Skin friction coefficients were also observed to increase with magnetic and porous parameters which could be attributed to higher resistance to flow in MHD. In summary, the findings demonstrate that hybrid nanofluids have higher thermal transport potential, though their efficiency is effectively reduced by magnetic, radiative, and porous factor. The conclusions derived from this work could be utilized for designing efficient thermal management systems, coating and material processing techniques, and electromagnetic flow control in various other applications. Future analyses may consider tri-hybrid nanofluids and variable property effects, or perhaps utilize machine-learning based methodology for optimizing design in real-time thermal system.

References

- [1] Choi, S. U. S., & Eastman, J. A. (1995). *Enhancing thermal conductivity of fluids with nanoparticles*. ASME International Mechanical Engineering Congress.
- [2] Hayat, T., & Alsaedi, A. (2018). *Magnetohydrodynamic flow of hybrid nanofluids over an exponentially stretching surface*. *International Journal of Heat and Mass Transfer*.
- [3] Ghadikolaei, S. S., et al. (2020). *Radiation effects on MHD nanofluid flow over an exponential sheet*. *Applied Mathematics and Computation*.
- [4] Reddy, J. N., et al. (2023). *Hybrid nanofluid heat transfer in porous exponential sheets with magnetic field and radiation effects*. *Alexandria Engineering Journal*.
- [5] Computational study of MHD tri-hybrid ($\text{Al}_2\text{O}_3 + \text{CuO} + \text{TiO}_2$)/ H_2O nanofluid flow between disk and cone with the effect of thermal radiation — Rashid A., Raizah Z., Alduais F.S., et al. *J. Thermal Analysis & Calorimetry*, 2025.
- [6] EMHD Flow and Heat Transfer of a Nanofluid Layer and a Hybrid Nanofluid Layer in a Horizontal Channel with Porous Medium — Nikodijević Đorđević, M.D.; Petrović J.D.; Kocić M.M.; Stamenković Ž.M.; Nikodijević D.D. *Applied Sciences*, Vol 15 (18), 2025.
- [7] Entropy generation on MHD motion of hybrid nanofluid with porous – stretching sheet — *Springer*, 2024.
- [8] Comparative numerical study between MHD Forchheimer nano and hybrid nanofluid flows over stretching sheet under aligned magnetic field — *Taylor & Francis*, 2024.

-
- [9] Thermal and velocity slip impacts on MHD tetra-hybrid nanofluids flowing past a stretching surface in a porous medium — *Springer*, 2025 (published 4 months ago).
- [10] Hayat, T., & Alsaedi, A. (2018). *MHD flow of nanofluids over a stretching surface with radiation*. **IJHMT**.
- [11] Ghadikolaei, S., et al. (2020). *MHD nanofluid flow with radiation and slip effects*. **Case Studies in Thermal Engineering**.
- [12] Waini, I., Ishak, A., & Pop, I. (2021). *MHD flow of a nanofluid past a porous sheet*. **Chinese J. Appl. Mech.**
- [13] Reddy, J. N., et al. (2023). *Hybrid nanofluid flow and heat transfer over an exponential porous sheet*. **Alexandria Engineering Journal**.
- [14] Khalil, S. (2024). *Study of hybrid nanofluid flow in a porous medium over an exponentially stretched sheet*. **Case Studies in Thermal Engineering**.
- [15] Rashid, A., et al. (2025). *Computational study of MHD tri-hybrid nanofluid flow under radiation*. **J. Thermal Analysis & Calorimetry**.
- [16] Nagaraja, B., Vidhya, K. G., Almeida, F., & Kumar, P. (2025). Numerical illustration of diffusive flow of blood-based tri-hybrid nanofluid generated by a curved stretching sheet using law of porosity. *Numerical Heat Transfer, Part A: Applications*, 86(16), 5626-5647.
- [17] Madiha Takreem, K., Venkateswarlu, B., Misra, A., Satya Narayana, P. V., & Harish Babu, D. (2025). Optimization of heat transfer characteristics of Casson hybrid nanofluid flow over a porous exponentially elongating surface using RSM approach. *Journal of Thermal Analysis and Calorimetry*, 150(3), 2133-2149.
- [18] Lone, S. A., Raizah, Z., Alrabaiah, H., Shahab, S., Saeed, A., & Khan, A. (2025). Exploring convective conditions in three-dimensional rotating ternary hybrid nanofluid flow over an extending sheet: a numerical analysis. *Journal of Thermal Analysis and Calorimetry*, 150(4), 2651-2666.
- [19] Lone, S. A., Al-Essa, L. A., Al-Bossly, A., Alduais, F. S., Khan, A., & Saeed, A. (2025). Thermal examination of chemically reactive Casson ternary hybrid nanofluid flow on bi-directional stretching sheet subject to Cattaneo–Christov mass/heat flux phenomena, variable porosity and exponential heat source. *Modern Physics Letters B*, 39(13), 2450496.
- [20] Arafat, H., Alosaimi, M., Ali, F., & Khidhir, D. M. (2025). Analytical study of the hybrid nanofluid for the porosity flowing through an accelerated plate: Laplace transform for the rheological behavior. *Applied Rheology*, 35(1), 20250057.